Energy density functional studies of elastic and inelastic scattering off nuclei

Michael Bender

Institut de Physique Nucléaire de Lyon, CNRS/IN2P3, Université de Lyon, Université Lyon 1
69622 Villeurbanne, France

work carried out while being at the

Centre d'Etudes Nucléaires de Bordeaux Gradignan, CNRS/IN2P3, Université de Bordeaux
33175 Gradignan, France

Workshop on
Electron-radioactive ion collisions: theoretical and experimental challenges
Espace de Structure Nucléaire et réactions Théorique, Saclay, 26 April 2016

What to expect from this talk

Bottom lines

- Method: Symmetry-restored Generator Coordinate Method based on deformed HFB states using an effective Skyrme interaction.
- Goal: study the impact of deformation, shape fluctuations and shape mixing (which all are "long-range" correlations) on observables.
- *no* in-medium ("short-range") correlations that are explicitely dealt with.

Outline

- What is a symmetry-restored Generator Coordinate Method based on deformed HFB states and why using it.
- Calculation of densities and transition densities in the laboratory frame
  – proof of principle.
- From simple to increasingly complicated MR schemes
  – possibilities for the future.

I assume you have heard about Hartree-Fock and Hartree-Fock Bogoliubov.

$\Rightarrow$ Single-Reference (SR) Energy Density Functional (EDF) Methods

Selfconsistent mean field

I assume you have heard about Hartree-Fock and Hartree-Fock Bogoliubov.

$\Rightarrow$ Single-Reference (SR) Energy Density Functional (EDF) Methods

I will talk about mixing HF & HFB states

$\Rightarrow$ Multi-Reference (MR) Energy Density Functional (EDF) Methods

Horizontal vs. vertical expansion of correlations

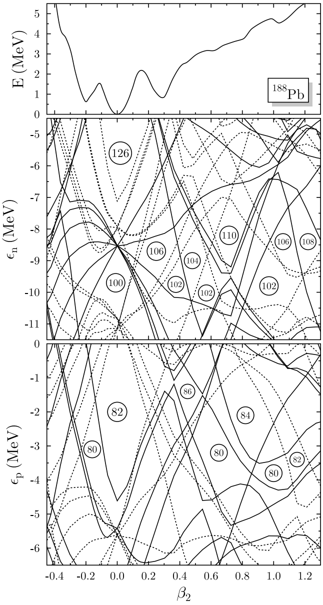

Horizontal vs. vertical expansion of correlations

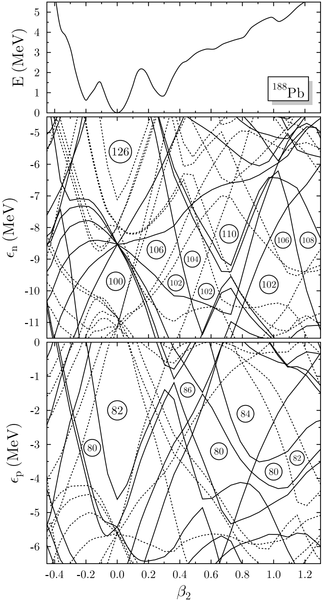

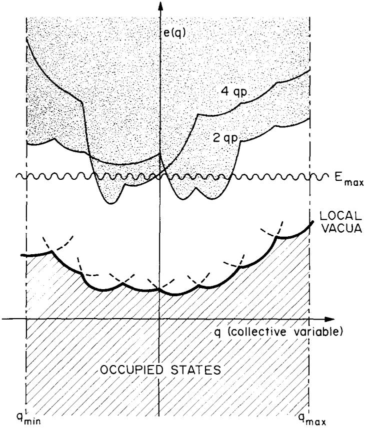

Fig. 1. Schematic plot of the energy versus the collective variable. The dark envelopes show the positions of the local vacua. The domain of the collective variable is defined by $q_{\min}$, $q_{\max}$ and the energy cut $E_{\max}$.

F. Dönau *et al*, NPA496 (1989) 333.

particle-number projector

$$\hat{P}_{N_0} = \frac{1}{2\pi} \int_0^{2\pi} d\phi_N \, \underbrace{e^{-i\phi_N N_0}}_{\text{weight}} \quad \overbrace{e^{i\phi_N \hat{N}}}^{\text{rotation in gauge space}}$$

angular-momentum restoration operator

$$\hat{P}^J_{MK} = \frac{2J+1}{16\pi^2} \int_0^{4\pi} d\alpha \int_0^{\pi} d\beta \, \sin(\beta) \int_0^{2\pi} d\gamma \, \underbrace{\mathcal{D}^{*J}_{MK}(\alpha,\beta,\gamma)}_{\text{Wigner function}} \quad \overbrace{\hat{R}(\alpha,\beta,\gamma)}^{\text{rotation in real space}}$$

K is the z component of angular momentum in the body-fixed frame.
Projected states are given by

$$|JMq\rangle = \sum_{K=-J}^{+J} f_J(K) \, \hat{P}^J_{MK} \, \hat{P}^Z \, \hat{P}^N \, |\mathrm{MF}(q)\rangle = \sum_{K=-J}^{+J} f_J(K) \, |JM(qK)\rangle$$

$f_J(K)$ is the weight of the component K and determined variationally

Axial symmetry (with the z axis as symmetry axis) allows to perform the α and γ integrations analytically, while the sum over K collapses, $f_J(K) \sim \delta_{K0}$

Configuration mixing by the symmetry-restored Generator Coordinate Method

Superposition of projected self-consistent mean-field states $|\mathrm{MF}(\mathbf{q})\rangle$ differing in a set of collective and single-particle coordinates $\mathbf{q}$

$$|NZJM\nu\rangle = \sum_{\mathbf{q}} \sum_{K=-J}^{+J} f_{J,\kappa}^{NZ}(\mathbf{q},K)\, \hat{P}_{MK}^{J}\, \hat{P}^{Z}\, \hat{P}^{N}\, |\mathrm{MF}(\mathbf{q})\rangle = \sum_{\mathbf{q}} \sum_{K=-J}^{+J} f_{J\nu}^{NZ}(\mathbf{q},K)\, |NZ\, JM(\mathbf{q}K)\rangle$$

with weights $f_{J\nu}^{NZ}(\mathbf{q},K)$.

$$\frac{\delta}{\delta f_{J\nu}^{*}(\mathbf{q},K)} \frac{\langle NZ\, JM\nu|\hat{H}|NZ\, JM\nu\rangle}{\langle NZ\, JM\nu|NZ\, JM\nu\rangle} = 0 \quad \Rightarrow \quad \text{Hill-Wheeler-Griffin equation}$$

$$\sum_{\mathbf{q}'} \sum_{K'=-J}^{+J} \left[\mathcal{H}_{J}^{NZ}(\mathbf{q}K,\mathbf{q}'K') - E_{J,\nu}^{NZ}\, \mathcal{I}_{J}^{NZ}(\mathbf{q}K,\mathbf{q}'K')\right]\, f_{J,\nu}^{NZ}(\mathbf{q}'K') = 0$$

with

$$\mathcal{H}_{J}(\mathbf{q}K,\mathbf{q}'K') = \langle NZ\, JM\, \mathbf{q}K|\hat{H}|NZ\, JM\, \mathbf{q}'K'\rangle \quad \text{energy kernel}$$
$$\mathcal{I}_{J}(\mathbf{q}K,\mathbf{q}'K') = \langle NZ\, JM\, \mathbf{q}K|NZ\, JM\, \mathbf{q}'K'\rangle \quad \text{norm kernel}$$

Angular-momentum projected GCM gives the

- correlated ground state for each value of J
- spectrum of excited states for each J

Numerical implementation

- full space of occupied single-particle states
- effective Skyrme interactions / energy density functionals
- “HF+BCS” or “HFB” solved with two-basis method
- Coordinate space representation on a 3d mesh using Lagrange-mesh technique

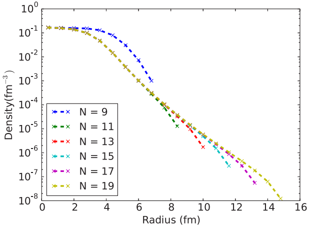

FIG. 9. (Color online) Radial density profile of ^{34}Ne in different box sizes with $dx = 0.8$ fm.

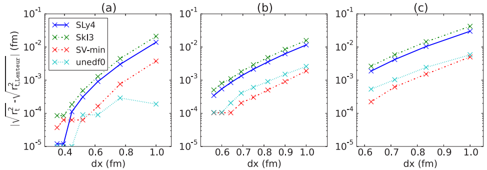

FIG. 10. (Color online) Absolute difference between the total rms radii calculated on a 3D mesh with respect to those of LENTEUR as a function of the step size dx for the spherical nuclei ^{40}Ca (a), ^{132}Sn (b), and ^{208}Pb (c) and those calculated with the Skyrme parametrizations as indicated.

W. Ryssens, P.-H. Heenen, M. B., PRC 92 (2015) 064318

Configuration mixing via the projected Generator Coordinate Method

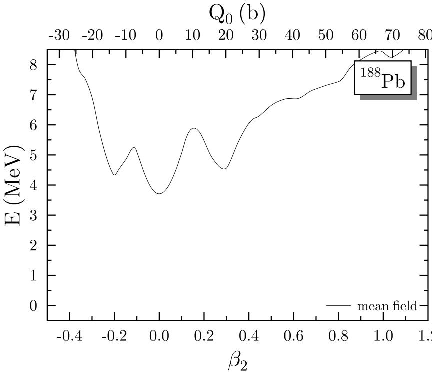

M. B., P. Bonche, T. Duguet, P.-H. Heenen, Phys. Rev. C 69 (2004) 064303.

Spectroscopy from MR EDF

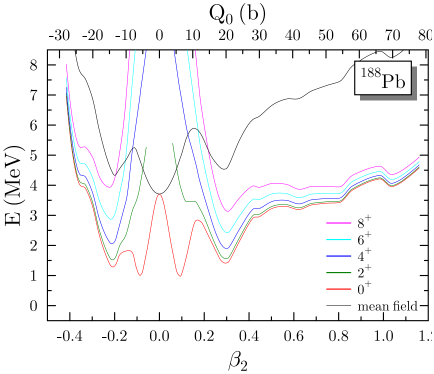

M. B., P. Bonche, T. Duguet, P.-H. Heenen, Phys. Rev. C 69 (2004) 064303.

Spectroscopy from MR EDF

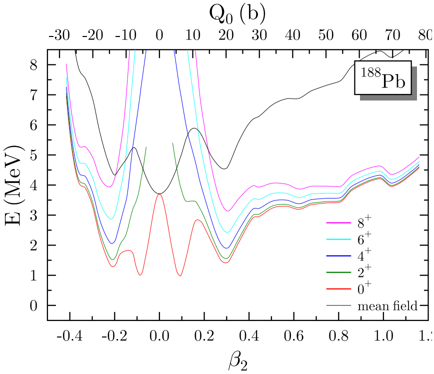

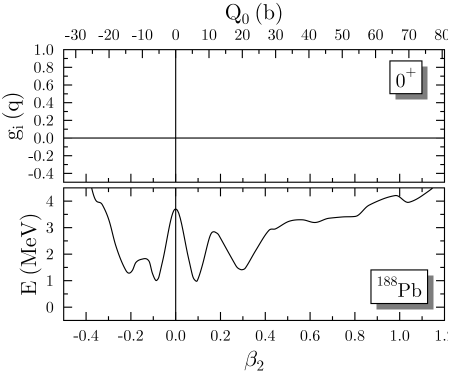

M. B., P. Bonche, T. Duguet, P.-H. Heenen, Phys. Rev. C 69 (2004) 064303.

Spectroscopy from MR EDF

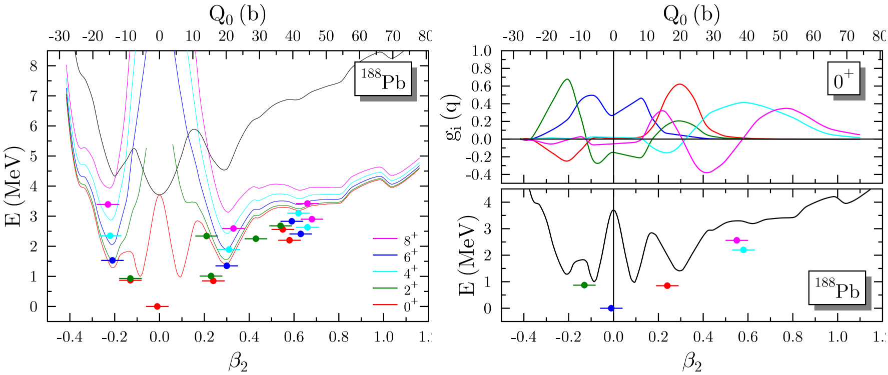

M. B., P. Bonche, T. Duguet, P.-H. Heenen, Phys. Rev. C 69 (2004) 064303.

Attention: $g_i^2(q)$ is not the probability to find a mean-field state with intrinsic deformation q in the collective state

M. B., P. Bonche, T. Duguet, P.-H. Heenen, Phys. Rev. C 69 (2004) 064303.
Experiment: T. Grahn *et al*, Phys. Rev. Lett. **97** (2006) 062501

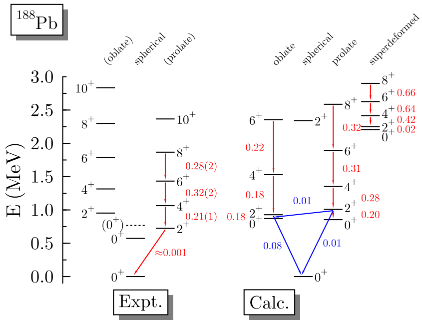

- in-band and out-of-band $E2$ transition moments directly in the laboratory frame with correct selection rules
- full model space of occupied particles
- only occupied single-particle states contribute to the kernels ("horizontal expansion")
- $\Rightarrow$ *no effective charges necessary*
- *no adjustable parameters*

$$B(E2; J'_{\nu'} \to J_\nu) = \frac{e^2}{2J'+1} \sum_{M=-J}^{+J} \sum_{M'=-J'}^{+J'} \sum_{\mu=-2}^{+2} |\langle JM\nu|\hat{Q}_{2\mu}|J'M'\nu'\rangle|^2$$

$$\beta_2^{(t)} = \frac{4\pi}{3R^2A}\sqrt{\frac{B(E2; J \to J-2)}{(J\,0\,2\,0\,|(J-2)\,0)^2 e^2}} \quad \text{with} \quad R = 1.2\,A^{1/3}$$

Spherical nuclei don't stay spherical "beyond the mean field"

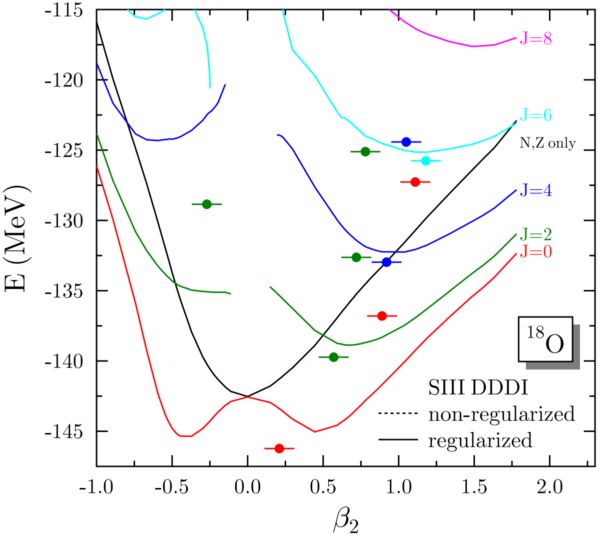

M. B., B. Avez, B. Bally, T. Duguet, P.-H. Heenen, D. Lacroix, unpublished

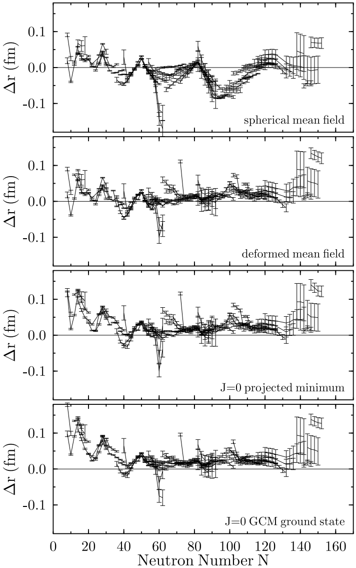

M. B., G. F. Bertsch, P.-H. Heenen, PRC 78 (2008) 054312

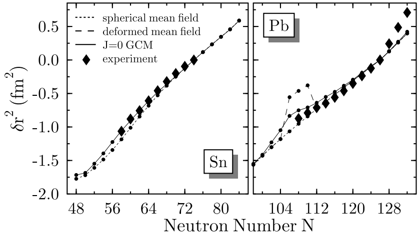

M. B., G. F. Bertsch, P.-H. Heenen, PRC 78 (2008) 054312

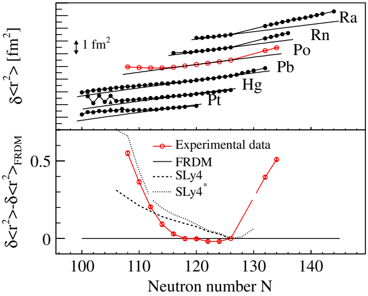

T. Cocolios, . . . , M. B., P.-H. Heenen, PRL 106 (2011) 052503.

Laboratory densities

Transition matrix element for tensor operator $\hat{T}^{\lambda}_{\mu} = \hat{a}^{\dagger}_{\mathbf{r}} \hat{a}_{\mathbf{r}} \, T^{\lambda}_{\mu}(\mathbf{r})$

$$\langle J_f M_f \nu_f | \hat{T}^{\lambda}_{\mu} | J_i M_i \nu_i \rangle \quad = \quad \int d^3 r \; \rho^{J_f M_f \nu_f}_{J_i M_i \nu_i}(\mathbf{r}) \; T^{\lambda}_{\mu}(\mathbf{r}) \, .$$

Transition density in the laboratory between GCM states $|J_i M_i \nu_i\rangle$ and $|J_f M_f \nu_f\rangle$ assuming axial HFB states

$$\rho^{J_f M_f \nu_f}_{J_i M_i \nu_i}(\mathbf{r}) \quad = \quad \sum_{q_f, q_i} f^{J_f *}_{\nu_f, q'} \, \langle q' | \hat{P}^{J_f}_{0 M_f} \, \hat{\rho}(\mathbf{r}) \, \hat{P}^{J_i \dagger}_{0 M_i} \, \hat{P}^N \, \hat{P}^Z | q \rangle \, f^{J_i 0}_{\nu_i, q}$$

with

$$\langle q' | \hat{P}^{J_f}_{0 M_f} \, \hat{\rho}(\mathbf{r}) \, \hat{P}^{J_i \dagger}_{0 M_i} \, \hat{P}^N \, \hat{P}^Z | q \rangle$$

$$= \frac{\hat{J}_i^2 \hat{J}_f^2}{(8\pi^2)^2} \int d\Omega' \; D^{J_f *}_{0 M_f}(\Omega') \sum_K D^{J_i}_{K0}(\Omega') \int d\Omega'' \; D^{J_i}_{0K}(\Omega'') \langle q' | \hat{\rho}(\tilde{\mathbf{r}}_{\Omega'}) \, \hat{P}^N \, \hat{P}^Z \, \hat{R}^{\dagger}(\Omega'') | q \rangle$$

$$\equiv \frac{\hat{J}_f^2}{8\pi^2} \int d\Omega' \; D^{J_f *}_{0 M_f}(\Omega') \sum_K D^{J_i}_{K M_i}(\Omega') \, \hat{R}^{\dagger}(\Omega') \, \rho^{J_f J_i K 0}_{q' q}(\mathbf{r})$$

For the density of the GCM state $|JM\nu\rangle$ one obtains

$$\rho^{JM\nu}_{JM\nu}(\mathbf{r}) \quad = \quad \sum_{q_f, q_i} f^{J*}_{\nu, q'} \, f^{J0}_{\nu, q} \sum_{\lambda} Y_{\lambda 0}(\hat{\mathbf{r}}) \, \langle JM\lambda 0 | JM \rangle \sum_K \langle J0\lambda K | JK \rangle \int \mathrm{d}\hat{\mathbf{r}}' \; \rho^{JJK0}_{q' q}(r, \hat{\mathbf{r}}') \; Y^{*}_{\lambda K}(\hat{\mathbf{r}}')$$

Pioneering mean-field work for ground states of spherical nuclei

PHYSICAL REVIEW C VOLUME 1, NUMBER 4 APRIL 1970

Structure of Finite Nuclei in the Local-Density Approximation*

J. W. Negele†‡
Laboratory of Nuclear Studies, Cornell University, Ithaca, New York 14850
(Received 25 August 1969)

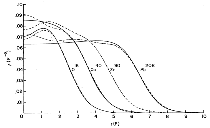

Fig. 6. Theoretical (dashed lines) and empirical (solid lines) charge-density distributions, including proton size and c.m. motion corrections. The empirical distributions for O^{16}, Ca^{40}, and Pb^{208} are from Refs. 72, 69, and 73, respectively.

PHYSICAL REVIEW C VOLUME 5, NUMBER 3 MARCH 1972

Hartree-Fock Calculations with Skyrme's Interaction. I. Spherical Nuclei*

D. Vautherin
Laboratory for Nuclear Science and Department of Physics, Massachusetts Institute of Technology, Cambridge, Massachusetts 02139,
and Institut de Physique Nucléaire, Division de Physique Théorique,† 91-Orsay, France
and
D. M. Brink
Department of Theoretical Physics, University of Oxford, Oxford, United Kingdom
(Received 15 November 1971)

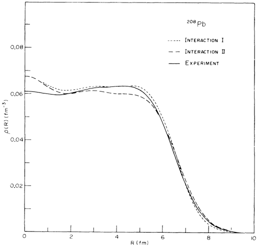

FIG. 6. Charge distribution of ^{208}Pb calculated with interactions I and II. The experimental charge distribution is that of Ref. 26.

PHYSICAL REVIEW C VOLUME 21, NUMBER 4 APRIL 1980

Hartree-Fock-Bogolyubov calculations with the *D*1 effective interaction on spherical nuclei

J. Dechargé and D. Gogny
Service de Physique Neutronique et Nucléaire, Centre d'Etudes de Bruyères-le-Châtel, Boîte Postale No. 561, 92542 Montrouge Cedex, France
(Received 3 August 1979)

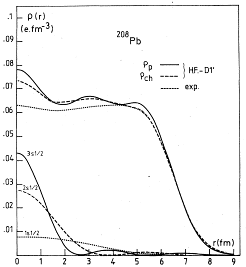

FIG. 13. The proton distribution ρ_p as well as the charge density distribution ρ_{ch} are plotted together with the density extracted from electron scattering experiment. In the lower part of the figure the contribution to the central density originating from the three $s^{1/2}$ HF states is also displayed.

PHYSICAL REVIEW C VOLUME 5, NUMBER 1 JANUARY 1972

Relativistic Self-Consistent Meson Field Theory of Spherical Nuclei

L. D. Miller* and A. E. S. Green
Department of Physics and Astronomy, University of Florida, Gainesville, Florida 32601
(Received 7 June 1971; revised manuscript received 12 October 1971)

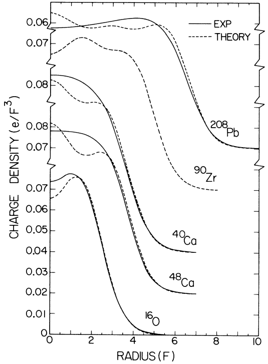

FIG. 1. Comparison of theoretical nuclear charge distributions with experimental (analytic) curves.

. . . using approximate angular-momentum projection ("rotational model"):

- Z. Zaringhalam and J. W. Negele, Nucl. Phys. A 288, 417 (1977).
- E. Moya de Guerra and A. E. L. Dieperink, Phys. Rev. C 18, 1596 (1978).
- E. Moya de Guerra and S. Kowalski, Phys. Rev. C 20, 357 (1979)
- E. Moya de Guerra and S. Kowalski, Phys. Rev. C 22, 1308 (1980).
- E. Moya de Guerra, Ann. Phys. (NY) 128, 286 (1980).
- M. Nishimura, D. W. L. Sprung, and E. Moya De Guerra, Phys. Lett. B 161, 235 (1985).
- E. Moya de Guerra, Phys. Rep. 138, 293 (1986).
- E. Graca, P. Sarriguren, D. Berdichevsky, D. W. L. Sprung, E. Moya De Guerra, M. Nishimura, Nucl. Phys. A 483, 77 (1988).
- D. Berdichevsky, P. Sarriguren, E. Moya de Guerra, M. Nishimura, and D. W. L. Sprung, Phys. Rev. C 38, 338 (1988).

. . . or using exact projection of HF states in a schematic single-particle basis:

- Y. Abgrall, P. Gabinski, and J. Labarsouque, Nucl. Phys. A 232, 235 (1974).

Densities and transition densities in the lab frame using exact projection

PHYSICAL REVIEW C **86**, 014310 (2012)

Beyond-mean-field study of the possible "bubble" structure of ^{34}Si

Jiang-Ming Yao,[1,2,*] Simone Baroni,[1,†] Michael Bender,[3,4,‡] and Paul-Henri Heenen[1,§]
[1]*Physique Nucléaire Théorique, Université Libre de Bruxelles, C.P. 229, B-1050 Bruxelles, Belgium*
[2]*School of Physical Science and Technology, Southwest University, Chongqing 400715, China*
[3]*Université Bordeaux, Centre d'Etudes Nucléaires de Bordeaux Gradignan, UMR5797, F-33175 Gradignan, France*
[4]*CNRS/IN2P3, Centre d'Etudes Nucléaires de Bordeaux Gradignan, UMR5797, F-33175 Gradignan, France*
(Received 10 May 2012; revised manuscript received 24 May 2012; published 9 July 2012)

PHYSICAL REVIEW C **91**, 024301 (2015)

Beyond-mean-field study of elastic and inelastic electron scattering off nuclei

J. M. Yao,[1,2,*] M. Bender,[3,4] and P.-H. Heenen[1]
[1]*Physique Nucléaire Théorique, Université Libre de Bruxelles, C.P. 229, B-1050 Bruxelles, Belgium*
[2]*School of Physical Science and Technology, Southwest University, Chongqing, 400715, China*
[3]*Université de Bordeaux, Centre d'Etudes Nucléaires de Bordeaux Gradignan, UMR5797, F-33175 Gradignan, France*
[4]*CNRS/IN2P3, Centre d'Etudes Nucléaires de Bordeaux Gradignan, UMR5797, F-33175 Gradignan, France*
(Received 9 October 2014; published 3 February 2015)

Laboratory densities of ^{34}Si

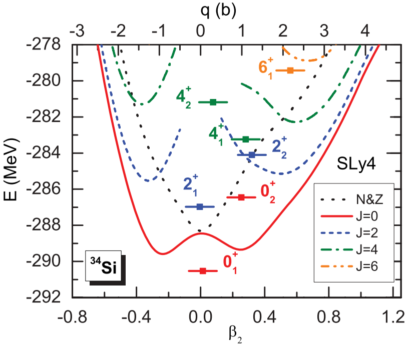

FIG. 1. (Color online) Energy curves for the particle-number-projected HFB states ($N\&Z$) and particle-number and angular-momentum projected states ($J = 0, 2, 4, 6$ curves) for ^{34}Si as a function of the intrinsic quadrupole deformation of the mean-field states they are projected from. The solid square dots correspond to the lowest GCM solutions, which are plotted at their average deformation $\sum_q q\,|g^J_\mu(q)|^2$ (see text).

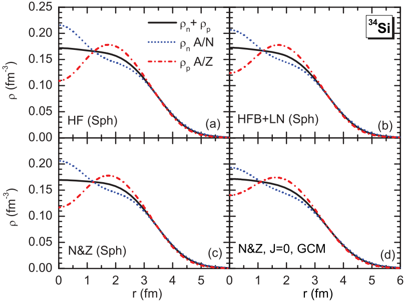

FIG. 5. (Color online) Neutron, proton, and total radial densities at $x = y = 0$ for ^{34}Si for the spherical HF state (a), the spherical HFB + LN state (b), and its projection on good particle numbers (c), as well as for the GCM 0^+_1 ground state (d). Neutron and proton densities have been rescaled with the factors A/N and A/Z, respectively.

J. M. Yao, S. Baroni, M. B., P.-H. Heenen, PRC 86 (2012) 014310

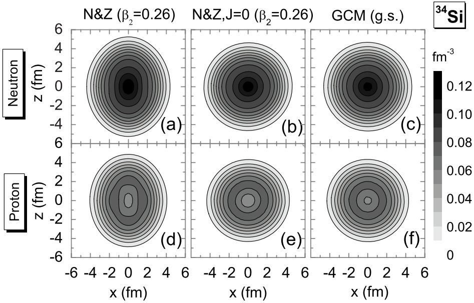

FIG. 6. Contour plots of the neutron (upper panels) and proton (lower panels) densities in the $y = 0$ plane for the particle number projected HFB + LN state with $\beta_2 = 0.26$ (left column), its projection on both particle numbers and total angular momentum $J = 0$ (middle column) and for the 0^+ GCM ground state (right column).

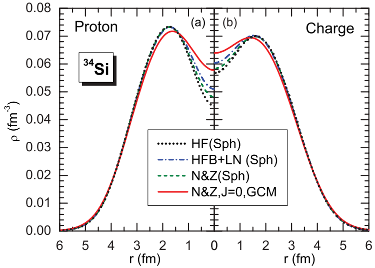

FIG. 7. (Color online) Comparison of point-proton densities (a) with the folded charge densities (b) for ^{34}Si for the same states as in Fig. 5.

J. M. Yao, S. Baroni, M. B., P.-H. Heenen, PRC 86 (2012) 014310

Physics Letters B 723 (2013) 459–463

Does a proton "bubble" structure exist in the low-lying states of ^{34}Si?

J.M. Yao [a,b,*], H. Mei [a], Z.P. Li [a]

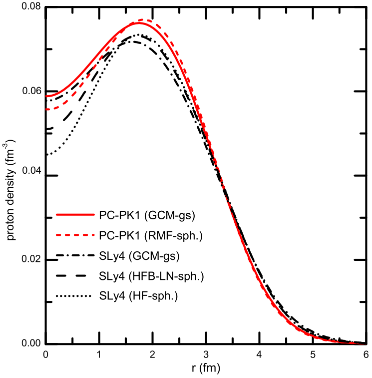

Fig. 4. (Color online.) Comparison of proton density distributions of ground state from both mean-field and beyond mean-field calculations for ^{34}Si. The non-relativistic results, taken from Ref. [9], are given for comparison.

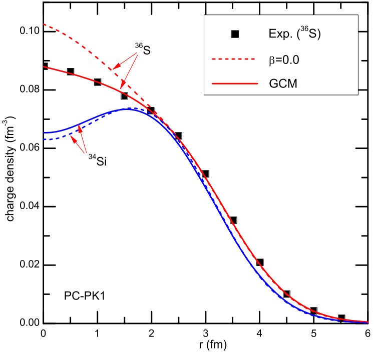

Fig. 5. (Color online.) Charge density distributions in ^{34}Si and ^{36}S from the relativistic calculations using the PC-PK1 force. The experimental data for ^{36}S are taken from Ref. [24].

Elastic and inelastic scattering off ^{24}Mg – densities

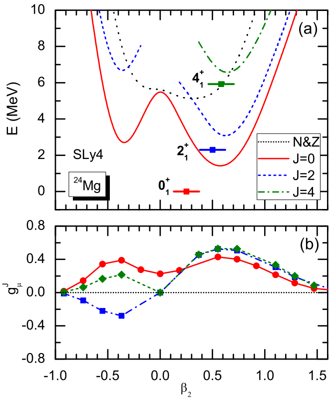

FIG. 1. (Color online) (a) Total energy (normalized to the 0_1^+ state) for the particle-number-projected HFB states (N&Z) and for the particle-number and angular-momentum-projected states (curves for $J = 0$, 2, and 4) for ^{24}Mg as a function of the intrinsic mass quadrupole deformation of the mean-field states. The solid squares indicate the lowest GCM solutions, which are plotted at their average deformation $\bar{\beta}_{J\mu}$. (b) Collective wave functions $g^J_{\mu,q}$ [cf. Eq. (5)] of the 0_1^+, 2_1^+, and 4_1^+ states.

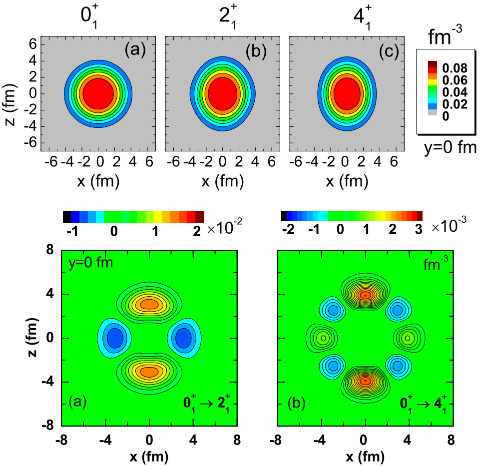

FIG. 3. (Color online) Contour plots of calculated TPD $\rho^{\alpha_f}_{0_1^+}(\mathbf{r})$, Eq. (21), in fm^{-3} in the $y = 0$ plane for the inelastic scattering from the ground state to the 2_1^+ (a) and the 4_1^+ (b) states with $M = 0$ in ^{24}Mg.

J. M. Yao, M. B., P.-H. Heenen, PRC 91 (2015) 024301

Elastic and inelastic scattering off ^{24}Mg – form factors

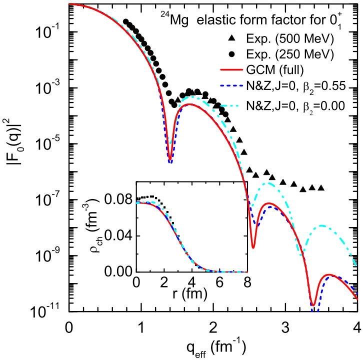

FIG. 4. (Color online) Elastic C0 form factor $|F_0(q)|^2$ for the 0_1^+ ground state of ^{24}Mg, in comparison with several calculations: he C0 form factor obtained by particle-number and $J = 0$ projection of a single HFB state with either $\beta_2 = 0$ (spherical shape; light blue dash-dotted curve) or $\beta_2 = 0.55$ (minimum of $J = 0$ projected energy curve; dark blue dashed curve) and from the full projected GCM calculation (red solid curve). The inset shows the corresponding charge density. Data (solid triangles and circles) are taken from Ref. [89].

J. M. Yao, M. B., P.-H. Heenen, PRC 91 (2015) 024301

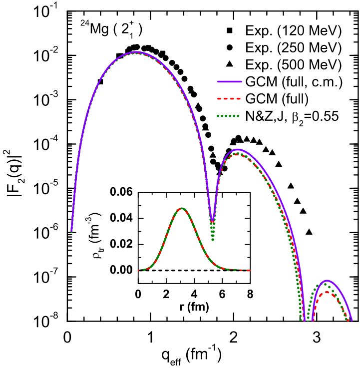

FIG. 5. (Color online) Longitudinal C2 form factor $|F_2(q)|^2$ for the transition from the ground state to the 2_1^+ state for ^{24}Mg, in comparison with available data. The form factor calculated with only one single configuration of $\beta_2 = 0.55$ and the form factor of the transition proton density from full GCM calculations are given for comparison. The inset shows the corresponding transition densities. Data are taken from Ref. [90] (squares) and Ref. [89] (circles and triangles).

Elastic and inelastic scattering off ^{58}Ni

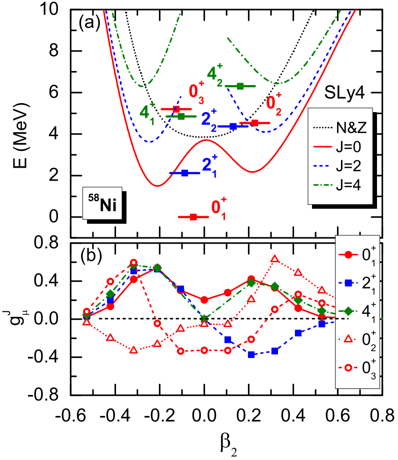

J. M. Yao, M. B., P.-H. Heenen, PRC 91 (2015) 024301

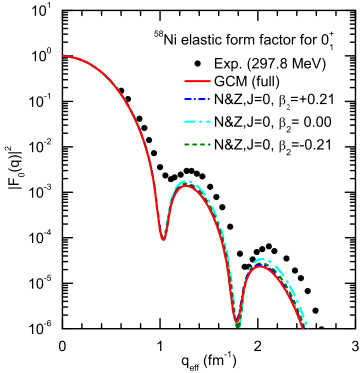

FIG. 10. (Color online) Data for the elastic form factor $|F_0(q)|^2$ for the ground state of ^{58}Ni taken from Ref. [99] in comparison with the form factor obtained from four different calculations: projection of a single HFB configuration with either $\beta_2 = 0$ (spherical shape) or $\beta_2 = \mp 0.21$ (oblate and prolate minima of the $J = 0$ energy curve) and full GCM of projected states.

Elastic and inelastic scattering off ^{58}Ni

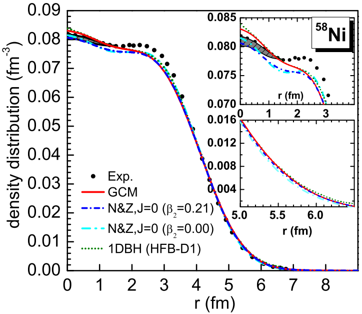

FIG. 11. (Color online) Comparison between the charge distribution of the ground state of ^{58}Ni obtained using single projected mean-field configurations or the full GCM basis and the experimental data [100]. A previous calculation using a one-dimensional Bohr Hamiltonian based on an HFB calculation with the Gogny D1 force (1DBH) [101] is also shown. The insets magnify the profile of the charge density at very small radii and in the nuclear surface.

J. M. Yao, M. B., P.-H. Heenen, PRC 91 (2015) 024301

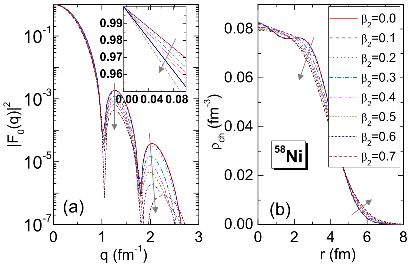

FIG. 12. (Color online) (a) Elastic form factor $|F_0(q)|^2$ for the $J = 0$ state of ^{58}Ni projected from a single HFB configuration with prolate deformation of β_2 increasing from 0.0 to 0.7, respectively. (b) Charge distributions corresponding to the form factors displayed in panel (a).

Elastic and inelastic scattering off Ni isotopes

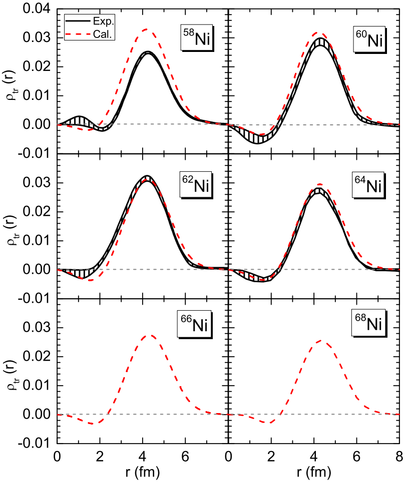

FIG. 17. (Color online) Calculated transition charge densities from the ground state to the 2_1^+ state for $^{58-68}$Ni, in comparison with available data [9].

J. M. Yao, M. B., P.-H. Heenen, PRC 91 (2015) 024301

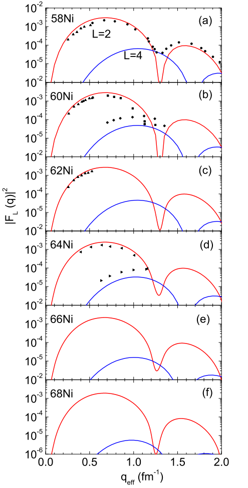

FIG. 18. (Color online) Calculated inelastic Coulomb form factors $|F_L(q)|^2$ for the transition from the ground state to the J_1^+ ($L = J = 2,4$) state in $^{58-68}$Ni, in comparison with available data, taken from Ref. [105] (up triangles), Ref. [106] (squares and diamonds), Ref. [107] (circles), and Ref. [108] (left and right triangles).

Other work (I'm aware of) published in the meantime

- X. Y. Wu, J. M. Yao, and Z. P. Li, Phys. Rev. C 89, 017304 (2014).
- H. Mei, K. Hagino, J. M. Yao, and T. Motoba, Phys. Rev. C 90, 064302 (2014).
- X.-Y. Wu and X.-R. Zhou, Phys. Rev. C 92, 054321 (2015).
- Y. Fukuoka, S. Shinohara, Y. Funaki, T. Nakatsukasa, and K. Yabana, Phys. Rev. C 88, 014321 (2013).

What could be done in the future: triaxiality, odd-A nuclei, ...

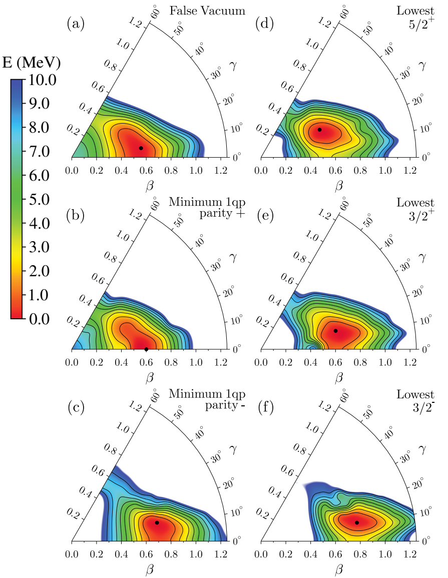

Angular-momentum and particle-number projected GCM of blocked triaxial one-quasiparticle states

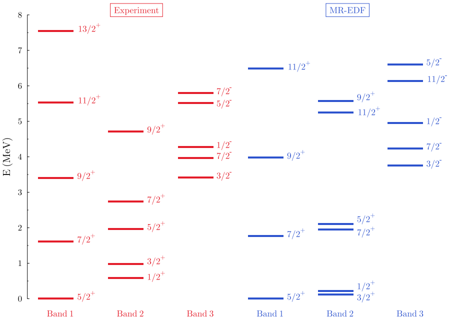

B. Bally, doctoral thesis, Université de Bordeaux (2014)

B. Bally, B. Avez, M. B., and P.-H. Heenen, PRL 113 (2014) 162501

Wrapping up

Take-away messages

- MR techniques provide useful tools to describe correlations related to the finiteness and self-boundedness of atomic nuclei
- symmetry restoration of symmetry-breaking reference states
- GCM-type mixing of (symmetry-restored) states
- Construction of laboratory densities, transition densities, and their form factors is feasible.

Questions to the audience

- What would be an interesting extension?
  - non-axiality?
  - single-particle excitations?
  - odd nuclei?
  - currents related to magnetic excitations?